Investigation of the electronic, linear and second-order nonlinear optical properties for the wide bandgap chalcopyrite ternary nitrides

L. C. Tang[a,b], Y.C. Chang[b,c], J. Y. Huang[a], and C. S. Chang[a]

[a]Department of Photonics & Institute of Electro-Optical Engineering, National Chiao Tung University, Hsinchu 305, Taiwan, ROC;
[b]Research Center for Applied Science, Academia Sinica, Taiwan, ROC;
[c]Department of Physics, University of Illinois at Urbana-Champaign, Urbana 61801 USA;

ABSTRACT

We present the results of the *ab initio* calculated electronic properties, first and second harmonic generation for the $A^{II}B^{IV}N_2$ (A^{II}=Be, Mg; B^{IV}=C, Si, Ge) compounds with chalcopyrite structure performed using the Linear Augmented Slater-Type Orbitals (LASTO) method. The second-order optical susceptibilities as functions of frequency for $A^{II}B^{IV}N_2$ are also presented. Specifically, we study the relation between the structural properties and the optical responses. Our electronic band structure and density of states (PDOS) analysis reveal that the underestimate bandgaps of these chalcopyrite $A^{II}B^{IV}N_2$ are wide enough (from $\tilde{4}$eV to $\tilde{6}$eV), direct transition and mainly located at Γ-point. Calcultion results show this new category wide-bandgap ternary nitrides has potential applications in optoelectronics.

Keywords: First-Principles, chi2, frequency-dependent, second-order optical susceptibilities

1. INTRODUCTION

$A^{II}B^{IV}N_2$ ($A^{II} = Be, Mg$, $B^{IV} = C, Si, Ge$) compounds are derived from III-V compounds by replacing the group-III element with group-II and group-IV elements. The atomic arrangement of the group-II and group-IV elements in II-IV-N2 compounds has ordered structure, and the symmetry changes from wurtzite to hexagonal structure with space group of Pna21 (pseudo-wurtzite structure).[1] Unfortunately, there were rare reseach results in II-IV-N2 compounds has symmetry changes from zinc-blende to chalcopyrite structure with space group of I-42d (pseudo-zinc-blende structure).[1] From the analogy of II-IV-P2 and/or II-IV-As2 compounds, chalcopyrite II-IV-N2 compounds are expected to have a large optical non-linearity, and thus, $A^{II}B^{IV}N_2$ has a potential for applications in optical band-pass and/or band-rejection filters, second harmonic generators, optical mixers, and parametric oscillators, as well as other chalcopyrite compounds.[2] Recently, epitaxial growth of ZnGeN2 was succeeded on GaN/sapphire[3] or sapphire substrates,[4] and absorption edge, excitonic luminescence, and its temperature dependence were reported.[5,6] $A^{II}B^{IV}N_2$ ($A^{II} = Be, Mg$, $B^{IV} = C, Si, Ge$) compounds, however, have not been well investigated. In this work, we studied the electronic band structures, linear and nonlinear optical responses such as the complex dielectric functions and the frequency-dependent $\chi^2_{ijk}(-2\omega;\omega,\omega)$ susceptibilities have been investigated by means of the Linear Augmented Slater-Type Orbitals (LASTO) method. The anisotropy of optical properties for $A^{II}B^{IV}N_2$ was also investigated.

Our calculations for the nonlinear response functions are based on the formalism given by Sipe and Ghahramani and by Aversa and Sipe.[7] The independent particle approximation has been used. This approach has the advantage that the response coefficients are inherently free of any unphysical divergences at zero frequency. It does not need to invoke the 'Sum rules' to eliminate the artificial divergences. The recent work of Dal Corso and Mauri,[8] based on an elegant Wannier function approach, is also free of such divergences.

Further author information: (Send correspondence to Li-Chuan Tang)
L. C. Tang: E-mail: newton4538.eo85g@nctu.edu.tw, Telephone: +886 3 380 4538
C.S. Chang: E-mail: cschang@nctu.edu.tw, Telephone: +886 3 571 2121

Photonic Fiber and Crystal Devices: Advances in Materials and Innovations in Device Applications II, edited by Shizhuo Yin, Ruyan Guo,
Proc. of SPIE Vol. 7056, 705605, (2008) · 0277-786X/08/$18 · doi: 10.1117/12.791577

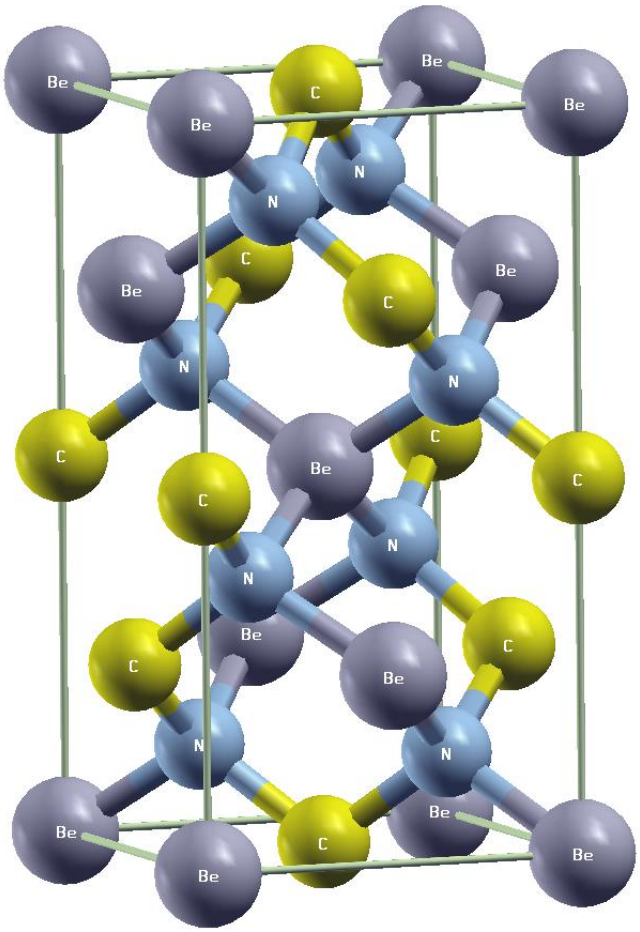

Figure 1. The crystal structure of tetragonal chalcopyrite

The full band structure calculation in this work utilized the full-potential Augmentd wave within the local density approximation (LDA). This method has an advantage over that employed by Moss and co-workers[9–13] in that it is first principles rather than semiempirical in nature. Huang and Ching[14–16] neglect the 'scissors' modification in the matrix elements; based on the evidence,[17] and the results of our own calculations, this did not much influence the tendency in the determination of the response functions. The local field effects in this work has not been included, since we do not expect such effects to lead to significant corrections for the materials considered here at the level of second-order response, as suggested by the work of Levine and Allan[17] . However, the inclusion of local field effects can be done in a straightforward way within our formalism for the response functions.

2. METHODS OF SIMULATION

The crystal structure of the tetragonal chalcopyrite, $A^{II}B^{IV}N_2$, is shown in Fig. 1. The unit cell exhibits $I\bar{4}2d$ symmetry ($a = b \neq c$, $\alpha = \beta = \gamma = 90^o$),[18,19] which can be considered as a superstructure of two zinc-blende structures. Four metal atoms A^{II}, B^{IV}, and eight crystallographically equivalent N atoms occupy the positions [(x, y, z); ($\bar{x}$,$\bar{y}$,$\bar{z}$); (y,$\bar{x}$,$\bar{z}$); ($\bar{y}$,x,$\bar{z}$); ($\bar{x}+1/2$, y,$\bar{z}+3/4$); ($x+1/2$,$\bar{y}$,$\bar{z}+3/4$); ($\bar{y}+1/2$,$\bar{x}$, $z+3/4$); ($y+1/2$, x, $z+3/4$)]. In chalcopyrite $A^{II}B^{IV}N_2$ ($A^{II} = Be, Mg$, $B^{IV} = C, Si, Ge$) crystals, metal atoms are tetrahedrally coordinated by N and vice versa. II-IV-V2 compounds have a large optical non-linearity, and they are promising

materials. ZnGeN2 is one of the II-IV-V2 compounds, and expected to be wide band gap and large difference of refractive index between ZnGeN2 and GaN from theoretical calculation. Moreover, $A^{II}B^{IV}N_2$ has small lattice mismatch to GaN for a-axis. However, optical properties of $A^{II}B^{IV}N_2$ are not clear. In this study, optical properties of single crystalline $A^{II}B^{IV}N_2$ were investigated.

The chalcopyrite structure showed two types of distortion, namely, tetragonal ($\eta = c/2a \neq 1$) and tetrahedral (an internal parameter u), with respect to the zinc-blende cubic structure.[?, 20, 21] The parameter u can be used to yield a measure of bond-length mismatch through the relation

$$(u - 0.25)^2 = \frac{d_{AN}^2 - d_{BN}^2}{a^2} \tag{1}$$

where the subscripts $A^{II} = Be, Mg$, $B^{IV} = C, Si, Ge$.

2.1. Computational Schemes

First principle simulations is a powerful tool to search for materials with specified properties, satifying the requirements of the most modern technology, when it is difficult to synthesize and investigate all kinds of compounds experimentally. The aim of our work is *ab initio* calculations of electronics and optical properties of $A^{II}B^{IV}N_2$ ($A^{II} = Be, Mg$, $B^{IV} = C, Si, Ge$) ternary compounds, and to estimate their prospects for applications.

The computer simulations performed included analysis and optimization of atomic arrangement in the crystal under consideration with subsequent calculation of their electronic and optical properties.

2.2. Electronic Properties

The obtained lattice parameters were used to calculate the electronic properties of $A^{II}B^{IV}N_2$. In order to understand the nature of optical transitions and other relevant effects on the calculated optical properties, an analysis of the local densities of states and other electronic properties of these $A^{II}B^{IV}N_2$ crystals were made. It was useful for extracting the local (atomic) information of the materials. Those radial pseudo atomic wavefunctions were the ones used to generate pseudopotentials and therefore, had the best consistency with the solved Bloch states. The projected values were equivalent to the coefficients of LCAO (Linear Combination of Atomic Orbitals) type expansion of original Bloch states using pseudo atomic orbitals as basis functions. The collection of those coefficients can be extracted local information from the system as a whole, where in the present work it is the PDOS (Partial or Projected Density of States) plots been used as an analysis tool. This atomic projection concept was then employed for resolving interesting components from total density of states (TDOS).

$$LDOS(\alpha, E) = \sum_n \sum_k \sum_l h_{nk,l}^{(\alpha)} \delta(E - E_{nk}) \tag{2}$$

The partial density states (PDOS) and local density of states (LDOS) could be used to provide valuable insight into the formation of energy bandgap and the nature of transitions from which the linear and nonlinear optical properties were originated.

$$PDOS(\alpha, l, E) = \sum_n \sum_k h_{nk,l}^{(\alpha)} \delta(E - E_{nk}) \tag{3}$$

2.3. Optical response functions

For the linear susceptibility, we adopt the analytic expression given by[2]

$$\tilde{\chi}_I^{ab}(-\omega; \omega) = \frac{e^2}{\Omega\hbar} \sum_{nm\mathbf{k}} f_{nm} \frac{r_{nm}^a(\mathbf{k}) r_{mn}^b(\mathbf{k})}{[\omega_{nm}(\mathbf{k}) + (\Delta/\hbar)(\delta_{mc} - \delta_{nc}) - \omega]}, \tag{4}$$

where n and m label energy bands; $f_{mn} \equiv f_m - f_n$, with f_i the Fermi occupation factor. $\mathbf{k}$ denote the wave vectors in the Brillouin zone. $\omega_{mn}(k) \equiv \omega_m(k) - \omega_n(k)$ denote the frequency differences. r_{mn} are the dipole matrix elements, which are related to the velocity matrix elements, v_{mn} via $r_{mn} = v_{mn}/(i\omega_{nm})$. Δ denotes the constant shift used in the 'scissors approximation' to correct the energy band gap difference caused by the local density approximation.

For the second-order response we write[2]

$$\chi^{abc}(-\omega_\beta - \omega_\gamma; \omega_\beta, \omega_\gamma) = \chi^{abc}_{II}(-\omega_\beta - \omega_\gamma; \omega_\beta, \omega_\gamma)$$
$$+\eta^{abc}_{II}(-\omega_\beta - \omega_\gamma; \omega_\beta, \omega_\gamma) + \frac{i}{(\omega_\beta + \omega_\gamma)}\sigma^{abc}_{II}(-\omega_\beta - \omega_\gamma; \omega_\beta, \omega_\gamma), \quad (5)$$

where χ^{abc}_{II} represents the purely interband contribution. η^{abc}_{II} describes the contribution from the modulation of the linear susceptibility by the intraband motion of the electrons. The third term is due to the modification of the intraband motion by the polarization energy associated with the interband transition. Explicit expressions for $\chi^{abc}(-2\omega : -\omega, -\omega)$ and $\chi^{abc}(-\omega : -\omega, 0)$ can be found in Appendix B of Ref.[2] To include the 'scissors operation' effect, we simply replace $\omega_{nm}(\mathbf{k})$ in these expressions by $\omega_{nm}(\mathbf{k}) + (\Delta/\hbar)(\delta_{mc} - \delta_{nc})$.

Band structures and optical properties of $A^{II}B^{IV}N_2$ (A^{II}=Be, Mg; B^{IV}=C, Si, Ge) compounds were calculated for the stable designed phase, chalcopyrite, by the Linear Augmented Slater-Type Orbitals (LASTO) method. The self-consistent procedure was performed on the grid of 1000 k-points uniformly distributed in the irreducible tetragonal BZ.

3. RESULTS AND DISCUSSION

Structural properties and the fundamental electronic and optical properties of the $A^{II}B^{IV}N_2$ (A^{II}=Be, Mg; B^{IV}=C, Si, Ge) compounds are presented in this section.

3.1. Structural properties

In Table 1, the six compounds were considered. The parameter *eta* in Berium ternary nitrides increased as the B-site cation were replaced from Carbon to Germanium. The

Table 1. Structural parameters, bond-lengths, and bulk modulus of the NLO crystals $A^{II}B^{IV}N_2$. The calculated values by using first-principles calculation with the supercell model were compared to the experimental values.

	$BeCN_2$	$BeSiN_2$	$BeGeN_2$	$MgCN_2$	$MgSiN_2$	$MgGeN_2$
$a(\mathring{A})$	3.710	4.100	4.250	4.110	4.6017	4.690
$c(\mathring{A})$	7.272	8.364	9.320	7.562	7.9120	9.890
$A^{II} - N(\mathring{A})$	1.7104	2.1681	2.2877	1.9181	2.1150	2.2399
$B^{IV} - N(\mathring{A})$	1.4957	1.5320	1.6446	1.5800	1.7280	1.9228
η	0.98	1.02	1.10	0.92	0.86	1.05
u	0.47	0.62	0.62	0.51	0.52	0.49

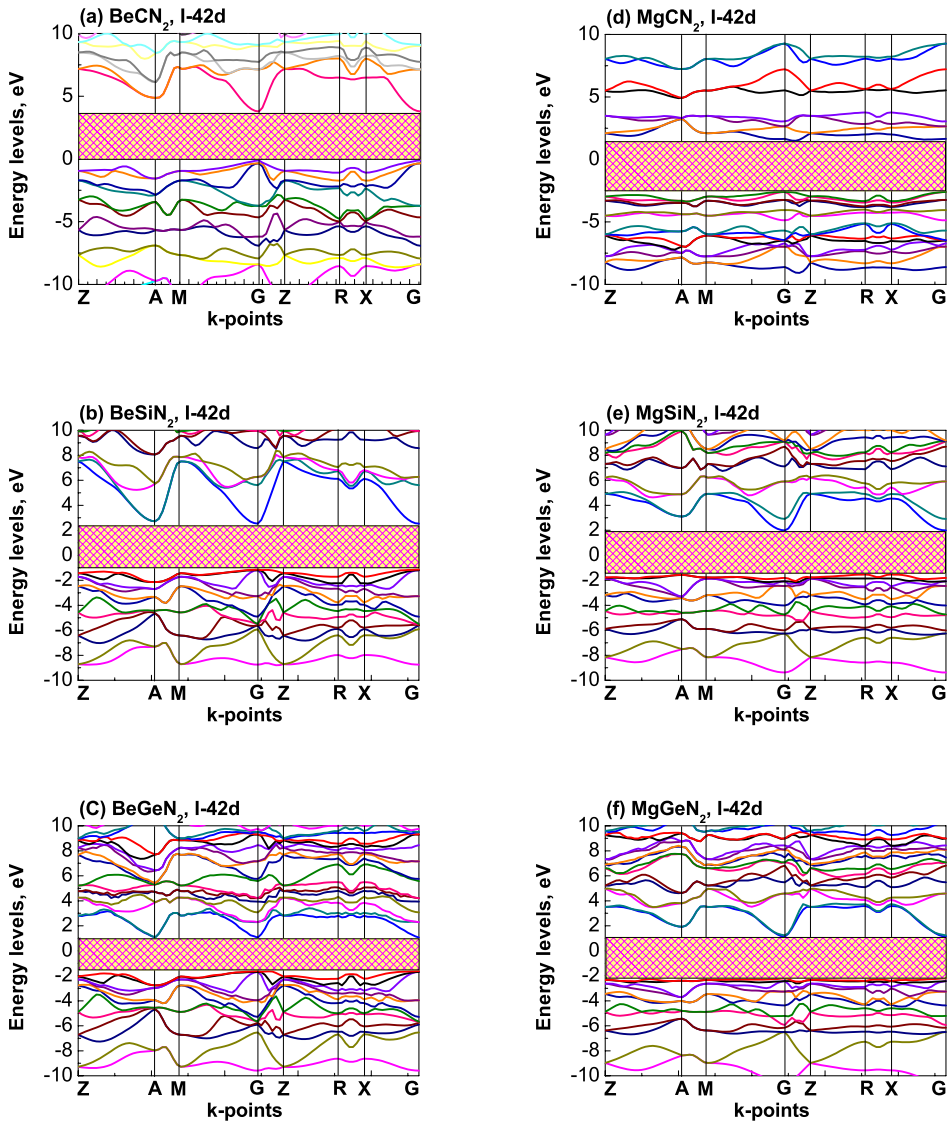

Figure 2. Electronoc band-structures of various chalcopyrite $A^{II}B^{IV}N_2$ (A^{II}=Be, Mg; B^{IV}=C, Si, Ge) with sapce group symmetry $I-42d$ (no. 122). They are (a)$BeCN_2$; (b)$BeSiN_2$; (c)$BeGeN_2$; (d)$MgCN_2$; (e)$MgSiN_2$; and (f)$MgGeN_2$;.

3.2. Electronic and optical properties

Figure 2 shows the electronic band structures for $A^{II}B^{IV}N_2$ (A^{II}=Be, Mg; B^{IV}=C, Si, Ge) obtained by using LASTO package. The figure 3 shows the corresponding projected density of states (PDOS). The calculated bandgap valuses varied from 2.68 eV ($BeGeN_2$) to 4.24 eV ($MgCN_2$), which were listed in the first row in Table 2. Because of the underestimation in bandgap in DFT scheme, these results should be adjusted to the higher values, from $\tilde{4}$ eV to $\tilde{6}$ eV.

Figure 4 shows the frequency-dependent linear optical properties for $A^{II}B^{IV}N_2$ (A^{II}=Be, Mg; B^{IV}=C, Si, Ge) obtained by using LASTO package. The calculated result also shows the anisotropic optical axis behavior and is consistent with the chalcopyrite structure characters. The anisotropic static $\chi^{(1)}_{xx}$ and $\chi^{(1)}_{zz}$ are shown in the second and third row in Table 2, respectively.

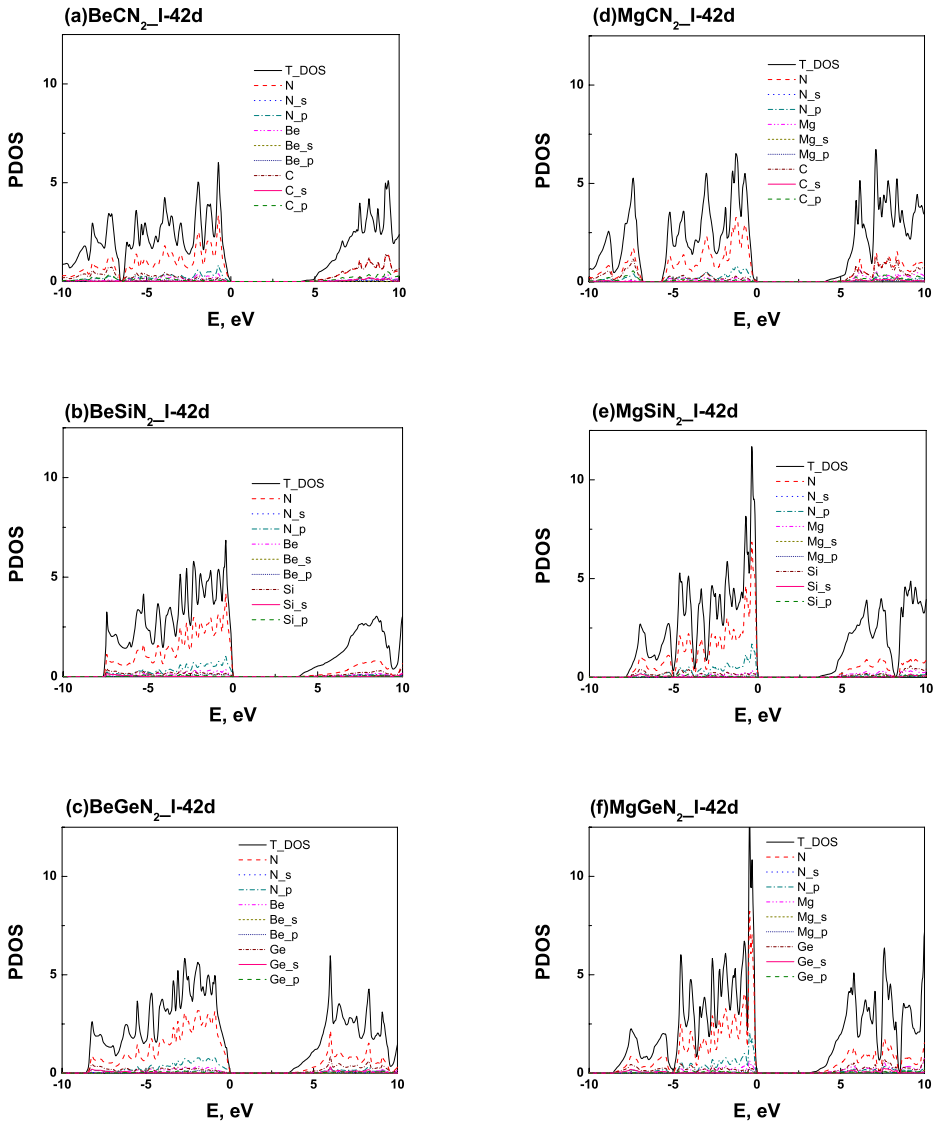

Figure 3. Density of State of various chalcopyrite $A^{II}B^{IV}N_2$ (A^{II}=Be, Mg; B^{IV}=C, Si, Ge) with sapce group symmetry $I-42d$ (no. 33). They are (a)$BeCN_2$; (b)$BeSiN_2$; (c)$BeGeN_2$; (d)$MgCN_2$; (e)$MgSiN_2$; and (f)$MgGeN_2$;.

The figure 5 shows the frequency-dependent second order optical susceptibilities. $BeGeN_2$ has the largest value among these chalcopyrite ternary nitrides. The nonvanished static $\chi^{(2)}_{xyz}$ and $\chi^{(2)}_{zxy}$ are shown in the forth and fifth row in Table 2, respectively.

4. CONCLUSIONS

We have reported the results of the *ab initio* calculated electronic properties, first and second harmonic generation for the $A^{II}B^{IV}N_2$ (A^{II}=Be, Mg; B^{IV}=C, Si, Ge) compounds with chalcopyrite structure performed using the Linear Augmented Slater-Type Orbitals (LASTO) method. The second-order optical susceptibilities as functions of frequency for $A^{II}B^{IV}N_2$ are also presented. $BeGeN_2$ has the lowest bandgap value and the highest nonlinear optical responses. Specifically, we study the relation between the structural properties and the optical

Table 2. The calculated bandgap values and optical susceptibilities in zero frequency of the NLO crystals $A^{II}B^{IV}N_2$ by using first-principle calculation.

	$BeCN_2$	$BeSiN_2$	$BeGeN_2$	$MgCN_2$	$MgSiN_2$	$MgGeN_2$
E_g,eV	3.90	3.67	2.68	4.24	3.79	3.33
$\chi^{(1)}_{xx}$	1.61	1.55	1.70	2.02	1.54	1.62
$\chi^{(1)}_{zz}$	1.64	1.56	1.70	2.23	1.59	1.68
$\chi^{(2)}_{xyz}$	12.49	6.45	18.45	16.19	8.39	16.78
$\chi^{(2)}_{zxy}$	12.62	6.47	15.02	15.07	7.68	15.24

responses. Our electronic band structure and density of states (PDOS) analysis reveal that the underestimate bandgaps of these chalcopyrite $A^{II}B^{IV}N_2$ are wide enough (from $\tilde{4}$eV to $\tilde{6}$eV) after re-estimation, direct transition and mainly located at Γ-point. Calcultion results show this new category wide-bandgap ternary nitrides has potential applications in optoelectronics.

ACKNOWLEDGMENTS

The authors are indebted to the financial support from the National Science Council of the Republic of China under both grants, NSC 96-2112-M-009-032 and NSC 95-2212-M-068-MY3. Address any correspondence to C. S. Chang. (cschang@mail.nctu.edu.tw) or L. C. Tang. (newton4538.eo85g@nctu.edu.tw).

REFERENCES

1. L.-C. Tang, C.-S. Chang, and J. Y. Huang *J. Phys.: Condens. Matter* **12**, p. 9129, 2000.
2. J. E. Sipe and E. Ghahramani *Phys. Rev. B* **48**, p. 11705, 1993.
3. P. Ren, J. Qin, and C. Chen *Inorganic Chemistry* **42**, pp. 8–10, 2003.
4. L. C. Tang, J. Y. Huang, C. S. Chang, M. H. Lee, and L. Q. Liu *J. Phys.: Condens. Matter* **17**, p. 7275, 2005.
5. V. M. Goldschmidt *Ber. Dtsch. Chem. Ges.* **60**, p. 1263, 1927.
6. V. M. Goldschmidt *Fortschr. Min.* **15**, p. 73, 1931.
7. C. Aversa and J. E. Sipe *Phys. Rev. B* **52**, p. 14636, 1995.
8. A. D. Corso and F. Mauri *Phys. Rev. B* **50**, p. 5756, 1994.
9. D. J. Moss, J. E. Sipe, and H. M. van Driel *Phys. Rev. B* **36**, p. 1153, 1987.
10. D. J. Moss, E. Ghahramani, J. E. Sipe, and H. M. van Driel *Phys. Rev. B* **41**, p. 1542, 1990.
11. E. Ghahramani, D. J. Moss, and J. E. Sipe *Phys. Rev. B* **43**, p. 8990, 1991.
12. E. Ghahramani, D. J. Moss, and J. E. Sipe *Phys. Rev. B* **43**, p. 9700, 1991.
13. D. J. Moss, E. Ghahramani, and J. E. Sipe *Phys. Status Solidi B* **164**, p. 587, 1991.
14. M. Z. Huang and W. Y. Ching *Phys. Rev. B* **45**, p. 8738, 1992.
15. M. Z. Huang and W. Y. Ching *Phys. Rev. B* **47**, p. 9464, 1993.
16. W. Y. Ching and M. Z. Huang *Phys. Rev. B* **47**, p. 9479, 1993.
17. Z. H. Levine and D. C. Allan *Phys. Rev. B* **44**, p. 12781, 1991.
18. S. C. Abrahams and J. L. Berstein *J. Chem. Phys* **59**, p. 1625, 1973.
19. B. Tell and H. M. Kasper *Phys. Trv* **B4**, p. 4455, 1971.
20. J. E. Jaffe and A. Zunger *Phys. Rev. B* **28**, p. 5822, 1984.
21. J. E. Jaffe and A. Zunger *Phys. Rev. B* **29**, p. 1882, 1984.

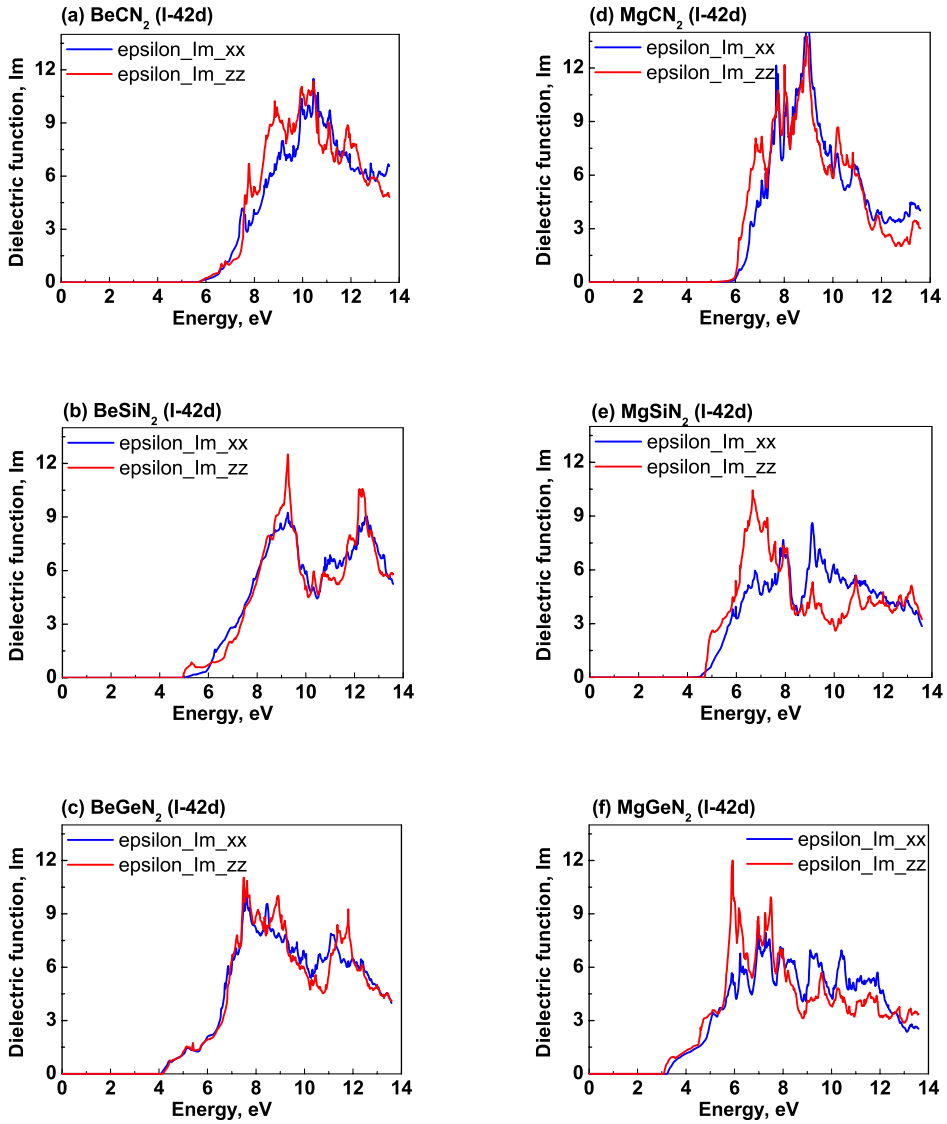

Figure 4. Dielectric functions of various tetragonal $A^{II}B^{IV}N_2$ (A^{II}=Be, Mg; B^{IV}=C, Si, Ge) with sapce group symmetry $I-42d$ (no. 122). They are (a)$BeCN_2$; (b)$BeSiN_2$; (c)$BeGeN_2$; (d)$MgCN_2$; (e)$MgSiN_2$; and (f)$MgGeN_2$;.

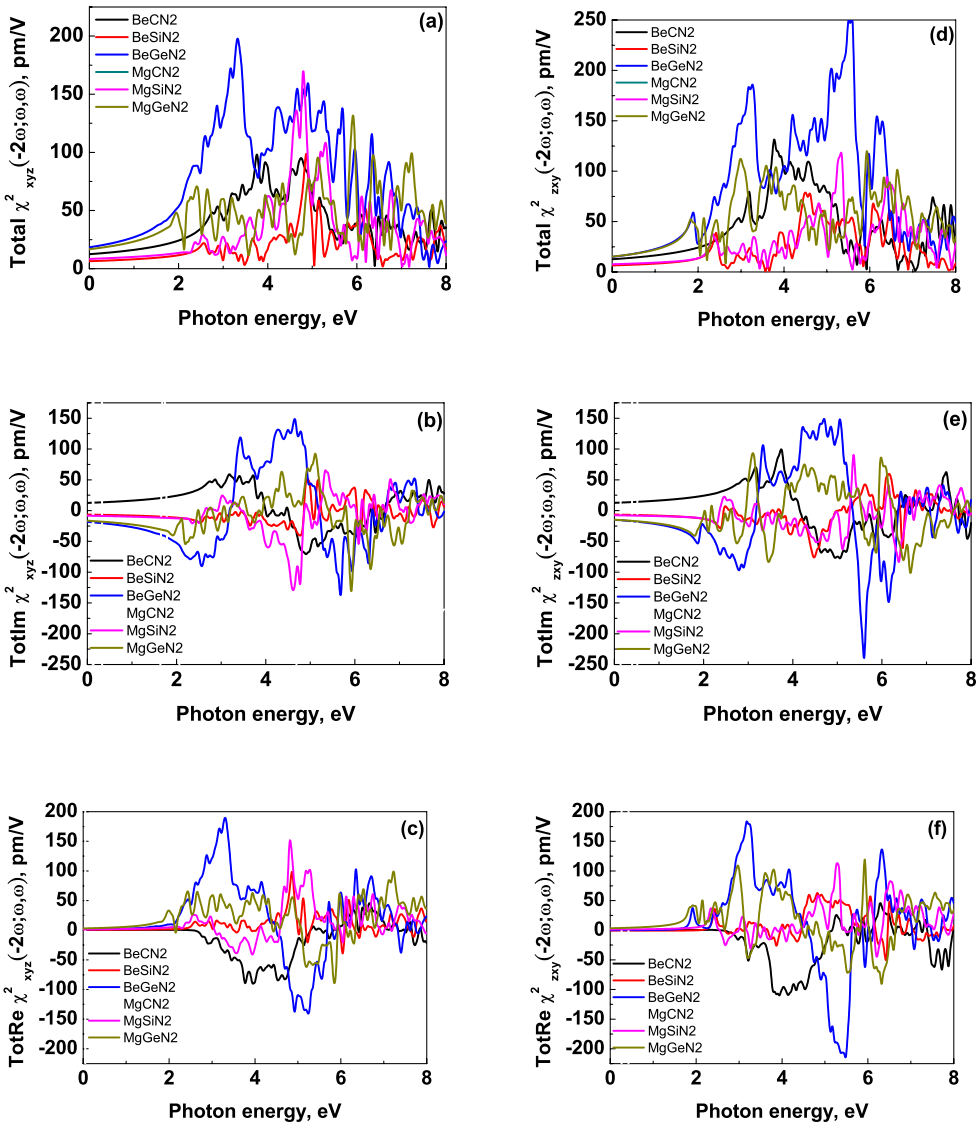

Figure 5. Frequency-dependent second order nonlinear susceptibilities of various tetragonal $A^{II}B^{IV}N_2$ (A^{II}=Be, Mg; B^{IV}=C, Si, Ge) with sapce group symmetry $I-42d$ (no. 122). They are (a)Total $\chi^2_{xyz}(-2\omega;\omega,\omega)$ responses; (b)Totally imaginary $\chi^2_{xyz}(-2\omega;\omega,\omega)$ responses; (c)Totally real $\chi^2_{xyz}(-2\omega;\omega,\omega)$ responses; (d)Total $\chi^2_{zxy}(-2\omega;\omega,\omega)$ responses; (e)Totally imaginary $\chi^2_{zxy}(-2\omega;\omega,\omega)$ responses; (f)Totally real $\chi^2_{zxy}(-2\omega;\omega,\omega)$ responses.